

Change in Electronic Properties of Carbon Nanotubes Caused by Local Distortion under Axial Compressive Strain

Ken Suzuki, Masato Ohnishi and Hideo Miura
 Fracture and Reliability Research Institute
 Graduate School of Engineering, Tohoku University
 Sendai, Japan
 kn@rift.mech.tohoku.ac.jp

Abstract—In this study, the change in electronic properties of carbon nanotubes (CNTs) under axial compressive strain was analyzed by using Green's function method based on tight-binding approach. A single (9, 0) CNT structure was used for the calculation. The column buckling of the CNT was occurred and a kink was formed in the buckled CNT with increasing compressive strain. After the formation of a kink, the local density of state (LDOS) at the energy higher than 0.3 eV was strongly localized in the buckled region. The conductance of the CNT with a kink was suppressed by the scattering of electrons due to the localization of LDOS. Therefore, electronic properties of the CNT changes drastically by buckling deformation when CNTs are subject to combined bending and axial compression.

Keywords—carbon nanotube; strain; buckling; conductance

I. INTRODUCTION

In any electronic devices composed of various materials, residual stress (strain) exists in the used materials due to large mismatches of both material properties and lattice constants between different materials. Of course, carbon nanotubes (CNTs) are subject to combined bending and axial load when CNTs are used and embedded in electronic devices such as transistors, interconnections and sensors and thus, three-dimensional complicated strain field exists in the CNTs. Since electronic properties of CNTs such as resistivity and the mobility of electrons are changed drastically under the application of mechanical stresses, it is very important to understand the effect of three-dimensional strain field on the electronic properties of CNTs for ensuring the stable operation and long-term reliability of electronic devices using CNTs.

Previous theoretical [1]-[3] and experimental [4], [5] studies have revealed that homogeneous axial and/or radial strain changes electronic properties of CNTs markedly. It is known that the change in the band gap of CNTs under uniaxial strain [1], [2] can be described by the cutting-line theory [6]. As for the homogeneous radial strain, originally metallic characteristics of armchair CNTs are shifted to semiconducting while their symmetry breaks under radial strain and the band gap of zigzag CNTs is changed by σ^* - π^* orbital hybridization. Therefore, both axial and radial strain change the electronic structure of the deformed CNT. Thus, the appearance of three-

dimensional complicated strain field caused by bending and buckling deformation should cause a large fluctuation of electronic properties of CNTs. However, the effect of three-dimensional local strain field on electric properties of CNTs still remains unclear because complicated orbital hybridization and change in the band gap occur simultaneously in the locally deformed CNTs.

In this study, in order to discuss the relationship between the local deformation of CNTs and their electronic properties, the change in electronic states of CNTs under uniaxial compressive strain, which induces the buckling deformation, was analyzed. Furthermore, the current through deformed CNTs was calculated using a four-orbital tight-binding based Green's function approach.

II. ANALYTICAL METHOD

A. Analysis Model

Geometric structures of (9, 0) CNTs under uniaxial compressive strain were obtained using a molecular mechanics (MM) and a molecular dynamics (MD) simulations. The adaptive intermolecular reactive bond order (AIREBO) potential [7] implemented in LAMMPS package [8] was used. Firstly, a relaxation calculation was performed to obtain a relaxation structure of a 9.4-nm-long (9, 0) CNT, which contains 22 primitive unit cells and 792 carbon atoms. Then, the primitive unit cells at the both ends were fixed and approached each other with the velocity of 0.2 m/s to apply a uniaxial compressive strain. The MD and MM simulations were used during the strain application and after the strain application to relax the geometric structure, respectively. In the MD simulation, a column and shell buckling (formation of a kink) deformations occurred at the compressive strain of 2.8% and 3.57%, respectively (the positive value indicates compressive strain). The examples of outlook just before and after the shell buckling are shown in Fig. 1. Under the strain of 0% to 2.7%, the CNT is deformed uniformly along the axial direction. At the strain of 2.8%, the middle section of the tube deviated from the center line, the dash-dot line and thus, column buckling of the CNT occurred. Then finally, a kink formed in the middle of the CNT (shell buckling) at the strain of 3.57%.

B. Analysis of Dihedral Angle in deformed CNT

In order to discuss the relationship between the geometric and the electronic structures, the distribution of dihedral angles in the strained CNT was analyzed. The π -orbital axis vector of atom i can be obtained by using the coordinates of its three nearest neighbor atoms [9].

$$V_{\pi,i} = \frac{V_{31} \times V_{21}}{|V_{31} \times V_{21}|}$$

where $V_{km} = V_m - V_k$ and V_k ($m, k = 1, 2, 3$) is the k -th nearest neighbor atom of i -th atom as shown in Fig. 2(a). Dihedral angle between atom i and j , θ_d , is given by

$$\theta_d = \cos^{-1} \left(\frac{V_{\pi,i} \cdot V_{\pi,j}}{|V_{\pi,i} V_{\pi,j}|} \right).$$

Figure 2(b) shows the pristine CNT with the π -orbital axis vector of each atom. As can be seen in this figure, there are two kinds of dihedral angle: the one along the circumference of the tube, and the one along the axis direction, which are 23° and 12° , respectively, for the pristine (9, 0) CNT.

C. Green's Function Method Based on Extended Tight-binding Approach

Using these deformed structures obtained from MM and MD calculations, the electronic transport properties were analyzed. Both ends of the deformed CNT are assumed to be attached to semi-infinite pristine CNTs as leads, i.e., strained region is held between left and right leads of unstrained pristine CNTs. The local density of states (LDOS) in the strained region was calculated using a tight-binding-based Green's function [10].

$$\text{LDOS}(E, r) = -\frac{1}{\pi} \text{Im}[G_s(E, r)],$$

where r is the position of an atom and G_s is the Green's function of the strained region. We employed the tight-binding potential of carbon as a function of the bond length [11]. The current through the strained region is obtained using the Landauer-Büttiker formula [12].

$$I(V) = \frac{2e}{h} \int dE T(E, V) [f_L(E - \mu_L) - f_R(E - \mu_R)],$$

where $T(E, V)$ is the transmission function through the strained region and f_L and f_R are the Fermi distributions of the semi-infinite pristine CNTs at the left and right ends. When a bias voltage V is applied to the strained region, the chemical potentials of the left and right leads, μ_L and μ_R , are assumed to be pinned at $-V/2$ and $V/2$. In addition, because obtaining the actual potential profile in the strained region is extremely time-consuming, the potential is assumed to drop linearly in the strained region.

III. CHANGE IN ELECTRONIC STATES UNDER UNIAXIAL COMPRESSIVE STRAIN

A. Effects of Buckling Deformation on Conductance

The change in the conductance under uniaxial compressive strain is shown in Fig. 3. The conductance curve of the pristine CNT shows a step structure. For the compressive strain lower

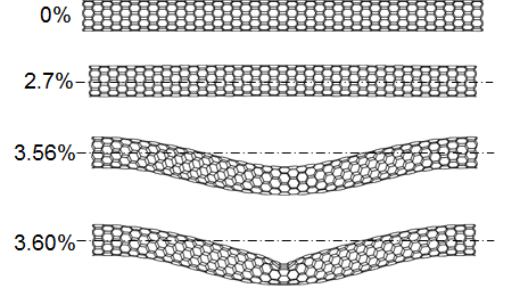


Fig. 1. Deformation behavior of a (9, 0) CNT under axial compressive strain

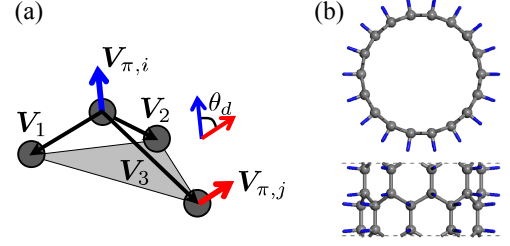


Fig. 2. (a) π -orbital axis vector obtained from the coordinates of three nearest neighbor atoms and (b) π -orbital axis vectors in a CNT

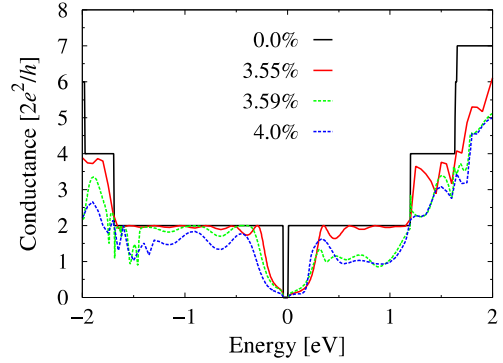


Fig. 3. Change in the conductance of a (9, 0) CNT under different amplitude of axial compressive strain

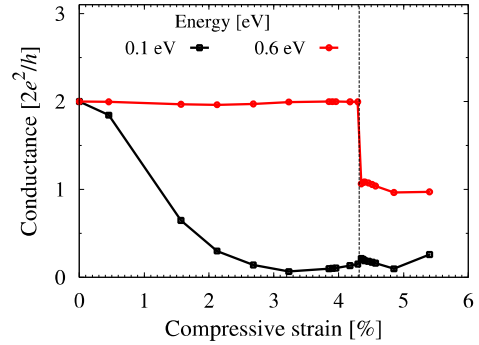


Fig. 4. Change in the conductance at the energy of 0.1 eV and 0.6 eV

than 3.57%, the decrease in the conductance is found in the low energy region around Fermi energy ($-0.3 \text{ eV} \leq E \leq 0.3 \text{ eV}$) and high energy region ($E \geq 1.2 \text{ eV}$). This decrease in the conductance near the Fermi level can be attributed to the effect of homogeneous uniaxial strain on the band gap of metallic CNTs. On the other hand, over 3.57% in which the kink formed in the tube as shown in Fig. 1, the conductance in the

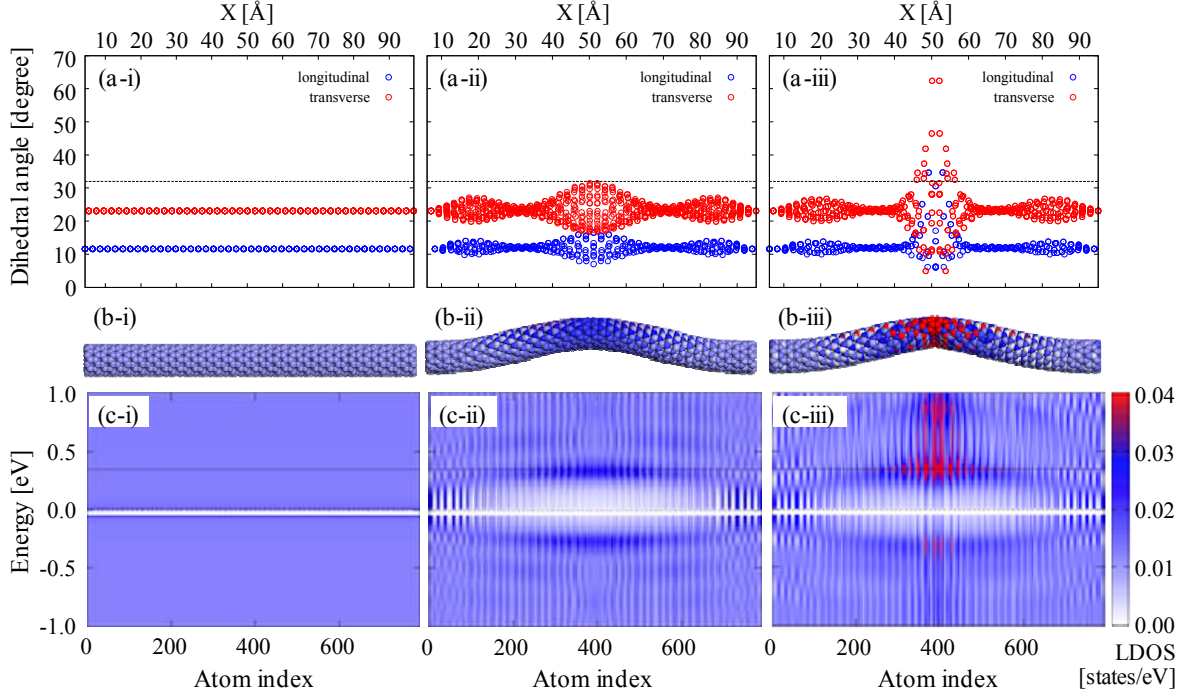


Fig. 5. Change in the distribution of (a) dihedral angle, (b) spatial distribution of the DOS at $E = 0.35$ eV, and (c) LDOS under (i) 0%, (ii) 3.56%, and (iii) 3.6% compressive strain

whole energy region decreases. Figure 4 shows the strain dependence of the conductance at representative energies of 0.1 eV and 0.6 eV. While the conductance at $E = 0.1$ eV decreases gradually in the compressive strain range from 0 to about 3%, the conductance at $E = 0.6$ eV drops sharply at the strain of 4.4%. This sharp decrease of the conductance was observed at the energy higher than 0.4 eV. Thus, the shell buckling deformation should cause a significant modification of the electronic properties of CNTs.

B. Change in Dihedral Angle and LDOS Distribution

The mechanism of the decrease in the conductance is discussed in terms of the change in the LDOS. Figure 5 shows the distribution (color contour) of dihedral angle, the DOS at $E = 0.35$ eV and LDOS in the range from -1 to 1 eV under 0%, 3.56% and 3.6% strain which corresponds to the pristine, column buckling and shell buckling state, respectively. In the pristine state, both the geometric and electronic parameters are distributed uniformly. When the compressive strain is applied to 3.56%, the LDOS in the vicinity of the Fermi energy decreases drastically and consequently, the band gap increases. Therefore, the decrease of the conductance in the low energy region (-0.3 eV $\leq E \leq 0.3$ eV) is attributed to the decrease of the LDOS around the Fermi energy.

In contrast to the effect of the column buckling, the shell buckling deformation affects the electronic states significantly. The LDOS at the energy higher than 0.3 eV is found to be strongly localized in the kink region after shell buckling. As we recently showed, the orbital hybridization in the low-energy region is introduced under homogeneous radial strain when the maximum dihedral angle in the CNT exceeds about 30° [13].

Therefore, when the number of dihedral angles exceeding this critical value is increased, the LDOS should also be localized significantly due to the orbital hybridization under local strain field. Here, the dotted lines in Fig. 5(a) denote the maximum dihedral angle in a CNT under 3.56% compressive strain, which can be considered the critical value. This figure clearly indicates that the number of dihedral angles exceeding the critical value is suddenly increased, caused by the shell buckling deformation. This localization of the LDOS occurred only when the shell buckling deformation occurred because the dihedral angle around the kink exceeded the critical value that introduces the localization. Generally, the localization of DOS induces scattering of electrons and thus, causes the drop of the conductance as seen in the change of conductance at $E = 0.6$ eV. Therefore, since the localization of the LDOS occurs due to the orbital hybridization in the buckled CNT, electronic properties of the CNT changes drastically by buckling deformation.

C. Change in Current Through Deformed CNTs

Finally, we analyzed the current through deformed CNTs by applying a tight-binding-based Green's function approach. Figure 6 shows the change in the current through the deformed CNTs under uniaxial compressive strain. With increasing bias voltage, the current value increased monotonically. Although the current did not change significantly when the bias voltage was less than 1.0 V, the change in the current through the deformed region was as follows in all cases. At the initial stage of strain loading, the current decreased by the compressive strain on bond lengths. Next, the current began to increase slightly during the column buckling deformation because the bond length was relaxed by the column buckling. Finally, the

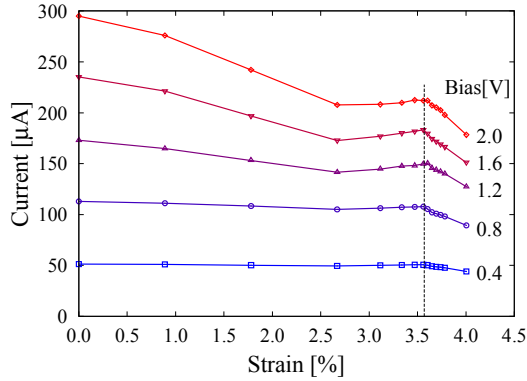


Fig. 6. Change in the current under uniaxial compressive strain

current decreased significantly because of the shell buckling deformation, which causes the localization of the LDOS and thus, electron scattering. Therefore, the effect of the localization of LDOS caused by the shell buckling deformation should dominate the change in electronic properties of CNTs in three-dimensional strain field.

IV. CONCLUSION

In this study, in order to understand the effect of the local strain field on the electronic properties of CNTs, the change in electronic properties of CNT under uniaxial compressive strain was analyzed by using Green's function method based on tight-binding approach. Discussing the relationship between the electronic states and geometric structures of deformed CNTs, we analyzed the effect of a uniaxial compressive strain in detail. When the shell buckling of the CNT occurred, the LDOS is strongly localized around a kink due to the orbital hybridization. This localization of the LDOS occurred only when the shell buckling deformation occurred because the dihedral angle in the buckled CNT exceeded the critical value which induces the localization. As a result, the localization of LDOS induces scattering of electrons and thus, causes drastic suppression of the conductance. Therefore, the effect of the localization of LDOS caused by the shell buckling should dominate the change in electronic properties of CNTs in three-

dimensional strain field and its effect is important factor for device application.

ACKNOWLEDGEMENT

This research was partly supported by the Grants-in-Aid for Scientific Research and the Japanese special coordination funds for promoting science and technology.

REFERENCES

- [1] L. Yang and J. Han, "Electronic Structure of Deformed Carbon Nanotubes," *Phys. Rev. Lett.*, vol. 85, no. 1, pp. 154–157, Jul. 2000.
- [2] L. Yang, M. Anantram, J. Han, and J. Lu, "Band-gap change of carbon nanotubes: Effect of small uniaxial and torsional strain," *Phys. Rev. B*, vol. 60, no. 19, pp. 13874–13878, Nov. 1999.
- [3] J. Q. Lu, J. Wu, W. Duan, F. Liu, B. F. Zhu, and B. L. Gu, "Metal-to-semiconductor transition in squashed armchair carbon nanotubes," *Phys. Rev. Lett.*, vol. 90, no. 15, p. 156601, 2003.
- [4] C. Stampfer, A. Jungen, R. Linderman, D. Oberfell, S. Roth, and C. Hierold, "Nano-Electromechanical Displacement Sensing Based on Single-Walled Carbon Nanotubes," *Nano Letters*, vol. 6, no. 7, pp. 1449–1453, Jul. 2006.
- [5] R. J. Grow, Q. Wang, J. Cao, D. Wang, and H. Dai, "Piezoresistance of carbon nanotubes on deformable thin-film membranes," *Appl. Phys. Lett.*, vol. 86, no. 9, p. 093104, 2005.
- [6] R. Saito, M. Fujita, G. Dresselhaus, and M. S. Dresselhaus, "Electronic structure of chiral graphene tubules," *Appl. Phys. Lett.*, vol. 60, no. 18, pp. 2204–2206, 1992.
- [7] D. W. Brenner, O. A. Shenderova, J. A. Harrison, S. J. Stuart, B. Ni, and S. B. Sinnott, *Journal of Physics: Condensed Matter*, vol. 14, p. 783, 2002.
- [8] LAMMPS Molecular Dynamics Simulator, <http://lammps.sandia.gov>
- [9] R. C. Haddon, "Comment on the Relationship of the Pyramidalization Angle at a Conjugated Carbon Atom to the σ Bond Angles," *J. Phys. Chem. A*, vol. 105, no. 16, pp. 4164–4165, Apr. 2001.
- [10] S. Datta, *Electronic Transport in Mesoscopic Systems* (Cambridge University Press, 1997).
- [11] D. Porezag, T. Frauenheim, T. Köhler, G. Seifert, and R. Kaschner, *Phys. Rev. B* 51, 12947, 1995.
- [12] M. Büttiker, Y. Imry, R. Landauer, and S. Pinhas, *Phys. Rev. B* 31, 6207, 1985.
- [13] M. Ohnishi, K. Suzuki, and H. Miura, *AIP Advances* 5, 047124, 2015.